

# Lead transport and binding by human erythrocytes in vitro

Timothy J. B. Simons

Physiology Group, Biomedical Sciences Division, King's College, Strand, London WC2R 2LS, UK

Received September 29, 1992/Received after revision and accepted December 2, 1992

**Abstract.** Transport and binding of  $\text{Pb}^{2+}$  by human erythrocytes were examined for cell Pb contents in the 1–10  $\mu\text{M}$  range, using the  $^{203}\text{Pb}$  isotope.  $\text{Pb}^{2+}$  crosses the erythrocyte membrane by the anion exchanger, and can also leave erythrocytes by a vanadate-sensitive pathway, identified with the  $\text{Ca}^{2+}$  pump. However,  $\text{Pb}^{2+}$  exit is very much less than expected from earlier experiments with resealed erythrocyte ghosts [Simons TJB (1988) *J Physiol (Lond)* 405:105–113] and the distribution of  $\text{Pb}^{2+}$  across the erythrocyte membrane is close to equilibrium. The high ratio of erythrocyte to plasma Pb seen in vivo appears to be due to the presence of a labile  $\text{Pb}^{2+}$ -binding component present in erythrocyte cytoplasm.

**Key words:** Erythrocyte – Red blood cell – Lead – Lead metabolism – Ethylmaltol

## Introduction

About 99% of the lead in human blood is associated with the erythrocytes, and 1% with the serum [4, 9]. The total amount present varies with environmental and occupational exposure. Blood lead levels have declined in recent years and values above 30  $\mu\text{g}/\text{dl}$  (1.5  $\mu\text{M}$ ) would now be regarded as high [8]. The distribution of lead between serum and erythrocytes must reflect the binding of lead to the molecules and cellular components present, and the transport of lead across the erythrocyte membrane. Lead can readily cross the erythrocyte membrane via the anion exchanger [14] but is also actively extruded from the cells by the  $\text{Ca}^{2+}$  pump [12, 15]. However, these experiments used extracellular free  $\text{Pb}^{2+}$  concentrations in the range from 10 nM to 4  $\mu\text{M}$ , which correspond to an erythrocyte lead content of at least 1 mmol/ $10^3$  cells, 1000-fold more than is found naturally. The aim of the present work was to reexamine the transport and binding of lead in human erythrocytes at much lower  $\text{Pb}^{2+}$  concentrations, approaching those

found in the population, and to try to account for the observed distribution of lead between serum and erythrocytes. Two approaches were used: (a) to study the equilibrium of tracer  $^{203}\text{Pb}$  when it is added to a suspension of erythrocytes in autologous serum and (b) to study the kinetics of transport and the equilibration of  $^{203}\text{Pb}$  for erythrocytes suspended in artificial medium in which the free  $\text{Pb}^{2+}$  concentration,  $[\text{Pb}^{2+}]$ , is buffered in the range 2–250 pM with nitrilotriacetic acid (NTA).

A preliminary account of this work has been published in abstract form [17].

## Materials and methods

**$^{203}\text{Pb}$  uptake for erythrocytes in serum.** Fresh human blood was divided into two unequal portions. One was heparinised, and washed several times with standard medium (145 mM KCl and 15 mM HEPES/KOH, pH 7.4 at 37° C), removing the leucocytes, to separate the erythrocytes. The other, larger portion, was allowed to clot, and serum was expressed. This procedure was adopted because anticoagulants, including heparin, bind  $\text{Pb}^{2+}$  [1]. Washed erythrocytes were resuspended in serum at about 20% haematocrit, the pH was adjusted to 7.4 at 37° C with HCl or NaOH, and 0.1–20  $\mu\text{M}$   $\text{Pb}(\text{NO}_3)_2$  (with  $^{203}\text{Pb}$ ) was added. Suspensions were incubated at 37° C for up to 3 h, and duplicate or triplicate samples of 100  $\mu\text{l}$  taken at specific times. The erythrocytes were separated by addition to 1.5-ml centrifuge tubes containing 0.8 ml “EDTA wash medium” (147.5 mM KCl, 5 mM HEPES/KOH, pH 7.4, and 1 mM EDTA/KOH) and 0.4 ml silicone fluid (sp. gr. = 1.07). After centrifuging at 12 000 rpm for 45 s, the supernatant fluids were removed and the tips of the tubes, containing the cell pellets, cut off and counted in a Nuclear Enterprises 8312 gamma counter. No correction was made for  $^{203}\text{Pb}$  in trapped extracellular fluid or bound extracellularly.  $^{203}\text{Pb}$  in serum was estimated by centrifuging samples of suspension and counting a known volume of supernatant. All counts were corrected for decay as the half-life of  $^{203}\text{Pb}$  is 52 h. In one of these experiments the basal  $\text{Pb}^{2+}$  concentration in the suspension before addition of  $^{203}\text{Pb}$  was found to be 0.06  $\mu\text{M}$  by atomic absorption spectrophotometry [14]. This corresponded to a cellular  $\text{Pb}^{2+}$  content of 0.2  $\mu\text{mol}/10^{13}$  cells.

**Other erythrocyte experiments.** Erythrocytes were separated from blood-bank blood as described previously [14], then usually preincubated for 2 h at 37° C in standard medium supplemented with

5 mM glucose and 5 mM inosine, to raise ATP levels. Sometimes cells were depleted of ATP by 2 h preincubation at 37° C in standard medium supplemented with 5 mM inosine and 5 mM iodoacetamide [5]. Cells were washed again after preincubation. In one experiment the basal  $Pb^{2+}$  concentration in washed blood-bank cells was measured by atomic absorption spectrophotometry [14] and found to be  $0.1 \mu\text{mol}/10^{13}$  cells.

**$^{203}Pb$  uptake/equilibrium.** Preincubated erythrocytes were suspended in standard medium plus (usually) 5 mM glucose, 1 mM NTA, 2.5–200  $\mu\text{M}$   $Pb(\text{NO}_3)_2$  and  $^{203}Pb$ , at 5% haematocrit, and incubated at 37° C. When bicarbonate was present,  $\text{KHCO}_3$  replaced an equal concentration of KCl. The pH of cell suspensions was usually adjusted to 7.4 after the start of incubation, by addition of HCl or KOH, because the  $[Pb^{2+}]$  in  $Pb^{2+}/\text{NTA}$  mixtures is highly sensitive to pH changes.  $[Pb^{2+}]$  was calculated from the data in [10], given for an ionic strength of 0.1 M and 25° C, but corrected to 37° C. The calculated apparent dissociation constant for  $Pb^{2+}/\text{NTA}$  at pH 7.4 was  $10^{-9.01}$  M, and for  $Pb^{2+}/\text{EGTA}$ ,  $10^{-10.87}$  M.

When needed, vanadate was added from a 200 mM stock solution ( $\text{Na}^+$  salt), to a final concentration of 4 mM. A high concentration was used because much of the vanadate is destroyed in incubations of 1 h or longer, seen by the disappearance of yellow colour in supernatants. Ethylmaltol is soluble in physiological media at 1 mM or 2 mM, but for convenience it was dissolved in ethanol at 500 mM and added to cell suspensions at the start of incubations. The final ethanol concentration was 0.2% or 0.4%.

Cells were sampled by addition of 0.5-ml portions of suspension to 1.5-ml centrifuge tubes containing 0.5 ml EDTA wash medium and 0.4 ml silicone fluid, then treated as above. When ethylmaltol was used, 1-ml portions of suspension were added to 0.4 ml silicone fluid, in order to avoid  $^{203}Pb$  redistribution before cell separation. The  $^{203}Pb$  in the cell pellet was corrected for trapped extracellular fluid in parallel control experiments, in which the cell suspensions were supplemented with 1 mM EDTA, which binds  $Pb^{2+}$  so strongly that its concentration would be below 1 fM [10]. The correction for trapped  $^{203}Pb$  was typically about 3%.

All cell concentrations are related to cell numbers, measured with a model ZF Coulter counter. They are expressed as the amount per  $10^{13}$  cells, which should be multiplied by 1.25 to give the amount per liter of cells, on the assumption of a mean cell volume of 80 fl.

**$^{203}Pb$  efflux from erythrocytes.** Erythrocytes were loaded with  $^{203}Pb$  by 2 h preincubation at 37° C in standard medium containing 25 mM  $\text{KHCO}_3$  and supplemented with  $^{203}Pb$  and either (a) 5 mM glucose, 5 mM inosine, 1 mM NTA and up to 50  $\mu\text{M}$   $Pb(\text{NO}_3)_2$  or (b) 5 mM inosine, 5 mM iodoacetamide, 1 mM 1,2-dihydroxybenzene-3,5-disulphonate (Tiron) and up to 20  $\mu\text{M}$   $Pb(\text{NO}_3)_2$ . Cells were then centrifuged, washed twice in ice-cold EDTA wash medium and resuspended in standard medium (without  $\text{HCO}_3^-$ ) at 5% haematocrit. Suspensions were incubated at 37° C and duplicate samples taken at intervals (usually 0, 20, 40 and 60 min), centrifuged, and efflux rate constants calculated from the appearance of  $^{203}Pb$  in the supernatant (see Fig. 6). A 2 mM solution of sodium vanadate was added to the final suspension to block the  $\text{Ca}^{2+}$  pump, and the vanadate-sensitive  $^{203}Pb$  efflux was calculated by multiplying the reduction in the efflux rate constant caused by vanadate by the cellular  $^{203}Pb$  content at the start of the efflux incubation.

**Materials.** Blood was supplied by the South London Regional Transfusion Centre and used not more than 14 days after donation.  $^{203}Pb$  was supplied by the MRC Cyclotron Unit, Hammersmith Hospital, London. Ethylmaltol was a gift of Professor R. C. Hider, Department of Pharmacy, King's College London.

**Curve fitting** was by the method of least squares using the software Multifit (Day Computing, Cambridge).

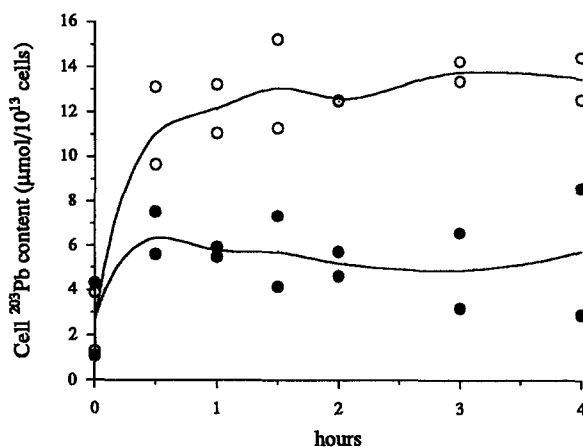


**Fig. 1.** Time course of  $^{203}Pb$  uptake by human erythrocyte suspended in autologous serum at pH 7.4 and 37° C (two experiments). At zero time 4  $\mu\text{M}$   $Pb(\text{NO}_3)_2$  (including  $^{203}Pb$ ) was added to erythrocyte suspensions of about 20% haematocrit, either under control conditions (○) or with 1 mM DIDS present (●). Duplicate samples were processed to measure cell  $^{203}Pb$  content at the times shown. The results of each experiment are shown separately. The extracellular  $^{203}Pb$  concentration in the period 1–3 h was measured as 0.6  $\mu\text{M}$  (○) or 2  $\mu\text{M}$  (●).

## Results

### *Equilibration of $^{203}Pb$ with erythrocytes suspended in serum*

When  $^{203}Pb$  is added to a suspension of erythrocytes in serum, it is rapidly taken up and in about 1 h reaches a steady state with a concentration ratio  $^{203}Pb_{\text{in}}/^{203}Pb_{\text{out}}$  of 20–30 (Fig. 1). Figure 1 also shows that 1 mM 4,4'-diisothiocyanatostilbene-2,2'-disulphonic acid (DIDS) reduces  $^{203}Pb$  uptake, suggesting an involvement of the anion exchanger [14]. A high concentration of DIDS was found to be necessary in serum, probably because of the binding of DIDS by albumin. In a subsidiary experiment (not shown) there was an  $\text{IC}_{50}$  of 1  $\mu\text{M}$  for DIDS inhibition of  $^{203}Pb$  uptake into blood-bank erythrocytes in a 10 mM  $\text{HCO}_3^-$  saline solution containing 115 pM  $Pb^{2+}$  (buffered with Tiron), but the  $\text{IC}_{50}$  was 9  $\mu\text{M}$  in the presence of 50 g/l bovine serum albumin.

The steady-state relationship between cell Pb and serum Pb was investigated by varying the amount of added Pb in the range 0.1–20  $\mu\text{M}$  (Fig. 2). The relationship is curvilinear and can be fitted by the combination of a straight line and a saturation curve (Fig. 2). At the lowest Pb concentrations (inset) the ratio  $^{203}Pb_{\text{in}}/^{203}Pb_{\text{out}}$  is about 40–50, corresponding to about 98% of the  $^{203}Pb$  being associated with the cells.

The serum  $Pb^{2+}$  concentration in Fig. 2 can be converted to the equivalent free  $Pb^{2+}$  concentration by dividing by 5200, the ratio of bound/free  $Pb^{2+}$  in serum [8]. Thus, the serum free  $Pb^{2+}$  concentration is estimated to be 192 pM at 1  $\mu\text{M}$  total  $Pb^{2+}$ , and about 6 pM at 0.03  $\mu\text{M}$  total  $Pb^{2+}$ , which corresponds to a cell  $Pb^{2+}$  content of 1  $\mu\text{mol}/10^{13}$  cells (Fig. 2 inset).

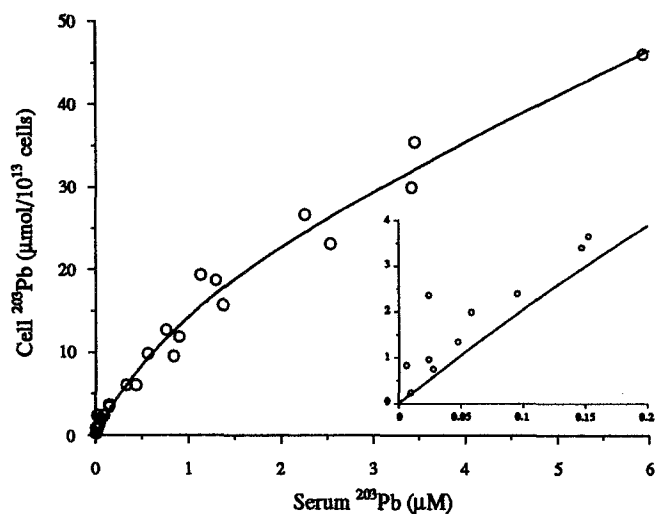


**Fig. 2.** Relationship between erythrocyte and serum  $^{203}\text{Pb}$  concentration. A 0.1–20  $\mu\text{M}$   $\text{Pb}(\text{NO}_3)_2$  solution (containing  $^{203}\text{Pb}$ ) was added to suspensions of erythrocytes in autologous serum. These were incubated at  $37^\circ\text{C}$  for 1 h, then cell and serum  $^{203}\text{Pb}$  were measured in triplicate. The line drawn is a least-squares fit to the equation  $y = ax + bx/(c + x)$  (i. e. linear + saturated), with parameters  $a = 4.8$ ,  $b = 20.9$ ,  $c = 1.2$ . The *inset* shows an expansion of the region close to the origin. Combined results of three experiments

#### Equilibration of $^{203}\text{Pb}$ with erythrocytes suspended in medium

In artificial media the free  $\text{Pb}^{2+}$  concentration can be controlled with  $\text{Pb}^{2+}$  buffers. NTA was used to give extracellular free  $\text{Pb}^{2+}$  concentrations in the range 2–250 pM. Two methods were used to equilibrate intracellular and extracellular  $\text{Pb}^{2+}$ .

**Bicarbonate experiments.** There was virtually no  $^{203}\text{Pb}$  uptake into cells suspended in  $\text{Pb}^{2+}/\text{NTA}$  buffers containing picomolar concentrations of  $\text{Pb}^{2+}$  unless bicarbonate was present (Fig. 3). The addition of 20  $\mu\text{M}$  DIDS completely prevented  $^{203}\text{Pb}$  uptake, as seen previously at higher  $\text{Pb}^{2+}$  concentrations [14]. On the other hand, 4 mM vanadate, which inhibits the  $\text{Ca}^{2+}$  pump and  $\text{Pb}^{2+}$  extrusion from erythrocytes [12, 15], enhances  $^{203}\text{Pb}$  uptake in the presence of bicarbonate (Fig. 3). This might indicate that the steady state reached after 3–4 h incubation at  $37^\circ\text{C}$  with bicarbonate (Fig. 3) represents a balance between influx and extrusion of  $\text{Pb}^{2+}$ .

**Ethylmaltol experiments.**  $^{203}\text{Pb}$  equilibration with 25 mM bicarbonate was fairly slow (Fig. 3), so an ionophore was sought to accelerate influx and to overcome any possible  $\text{Pb}^{2+}$  extrusion. Neither A 23187 nor ionomycin accelerated  $\text{Pb}^{2+}$  uptake (not shown), but ethylmaltol, which has previously been used as a  $\text{Zn}^{2+}$  ionophore [7], was found to be an effective  $\text{Pb}^{2+}$  ionophore. It dissociates in water, forming ethylmaltol $^-$  and  $\text{H}^+$ , and combines with divalent cations such as  $\text{Zn}^{2+}$  to form complexes  $\text{Zn}(\text{ethylmaltol})^+$  and  $\text{Zn}(\text{ethylmaltol})_2$ . (It does not carry  $\text{Ca}^{2+}$  or  $\text{Mg}^{2+}$ .) Ethylmaltol accelerates  $^{203}\text{Pb}$  uptake into erythrocytes. The rate of uptake in-

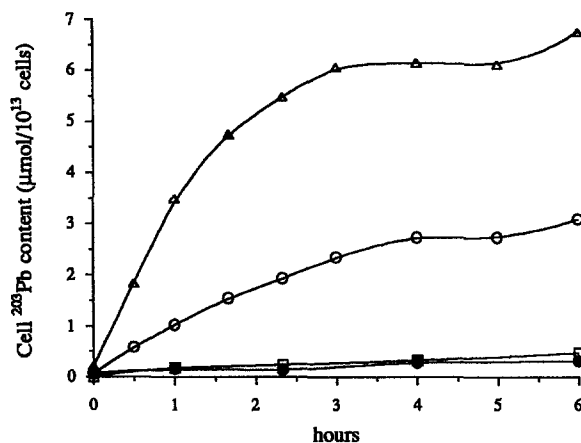


**Fig. 3.** Time course of  $^{203}\text{Pb}$  uptake by human erythrocytes suspended in  $\text{Pb}^{2+}/\text{nitrotriacetic acid}$  (NTA) buffers. Cells were suspended at 5% haematocrit and  $37^\circ\text{C}$  in a medium containing 15 mM HEPES/KOH, pH 7.4, 5 mM glucose, 1 mM NTA, 20  $\mu\text{M}$   $\text{Pb}(\text{NO}_3)_2$  and either ( $\square$ ) 145 mM KCl, ( $\circ$ ) 120 mM KCl and 25 mM  $\text{KHCO}_3$ , ( $\triangle$ ) 120 mM KCl and 25 mM  $\text{KHCO}_3$  plus 4 mM vanadate or ( $\bullet$ ) 120 mM KCl and 25 mM  $\text{KHCO}_3$  plus 20  $\mu\text{M}$  DIDS. The cell  $^{203}\text{Pb}$  was measured by taking duplicate samples at the times shown. One of three similar experiments

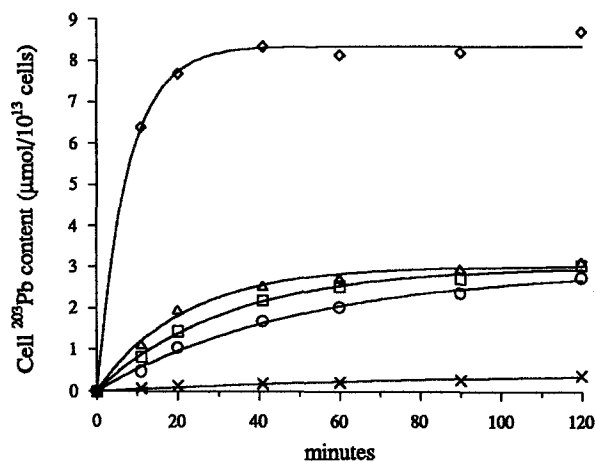


**Fig. 4.** Time-course of  $^{203}\text{Pb}$  uptake as a function of  $\text{Pb}^{2+}$  and ethylmaltol concentration.  $^{203}\text{Pb}$  uptake was measured at  $37^\circ\text{C}$  from solutions containing ( $\times$ ) 2.5 pM  $\text{Pb}^{2+}$  with 2 mM ethylmaltol, ( $\circ$ ) 4.9 pM  $\text{Pb}^{2+}$  with 1 mM ethylmaltol, ( $\square$ ) 4.9 pM  $\text{Pb}^{2+}$  with 2 mM ethylmaltol, ( $\triangle$ ) 4.9 pM  $\text{Pb}^{2+}$  with 4 mM ethylmaltol or ( $\diamond$ ) 13.5 pM  $\text{Pb}^{2+}$  with 2 mM ethylmaltol. Standard medium was used at pH 7.4, with  $\text{Pb}/\text{NTA}$  buffers, except at 13.5 pM  $\text{Pb}^{2+}$ , which used a  $\text{Pb}/\text{EGTA}$  buffer. Duplicate measurements were made except at 0 time, where the point has been plotted conventionally. The curves are least-squares fits to the equation  $y = A(1 - e^{-kt})$ . The calculated rate constants in  $\text{min}^{-1}$  are ( $\times$ ) 0.0126, ( $\circ$ ) 0.0195, ( $\square$ ) 0.0307, ( $\triangle$ ) 0.0455, ( $\diamond$ ) 0.13

creases with increasing concentrations of ethylmaltol and external  $\text{Pb}^{2+}$ . Figure 4 shows the time course of  $^{203}\text{Pb}$  uptake at low  $\text{Pb}^{2+}$  concentrations – the rate of  $^{203}\text{Pb}$  uptake was faster at higher concentrations (not shown). On the basis of these observations it was decided to incubate for 2 h with 2 mM ethylmaltol to reach a steady state when  $[\text{Pb}^{2+}]$  was below 20 pM, but to use a 1-h incubation and 1 mM ethylmaltol at higher  $\text{Pb}^{2+}$  concentrations.

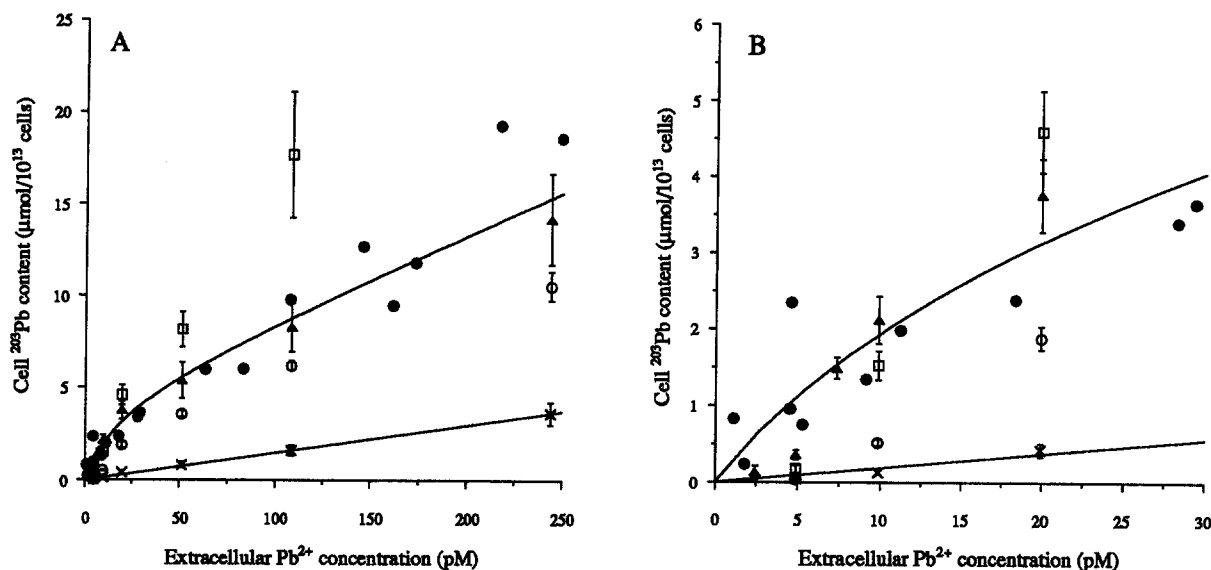


**Fig. 5 A, B.** Steady-state relationship between erythrocyte  $^{203}\text{Pb}$  and extracellular  $\text{Pb}^{2+}$  concentration. Observations were made in standard medium, supplemented with 1 mM NTA and 2.5–200  $\mu\text{M}$   $\text{Pb}(\text{NO}_3)_2$ , and are presented as mean  $\pm$  SEM of three to nine experiments, in each of which cell  $^{203}\text{Pb}$  was measured in triplicate after 1, 2 or 3 h incubation at 37 $^\circ$  C, as explained in the text.  $\circ$ , Cells in 25 mM  $\text{HCO}_3^-$ ;  $\square$ , in 25 mM  $\text{HCO}_3^-$  + 4 mM vanadate;  $\triangle$ , in  $\text{HCO}_3^-$ -free medium with 1 mM or 2 mM ethylmaltol;  $\times$ , ATP-depleted cells in  $\text{HCO}_3^-$  or ethylmaltol medium

(in this case  $n = 7-13$ ). The similar experiments with erythrocytes suspended in serum (Fig. 2) have also been superimposed ( $\bullet$ ). The data for ATP-depleted cells ( $\times$ ) have been fitted by the equation  $y = ax$ , with  $a = 0.0148$ , and for ATP-fed cells, ( $\triangle$ ) and ( $\bullet$ ) together, by the equation  $y = ax + bx/(c + x)$ , with  $a = 0.049$ ,  $b = 4.46$  and  $c = 20.1$ . Another ( $\square$ ) point at 74  $\mu\text{mol}/10^{13}$  cells and 244 pM  $\text{Pb}^{2+}$  is off the scale of graph A. **B** expands the scale close to the origin

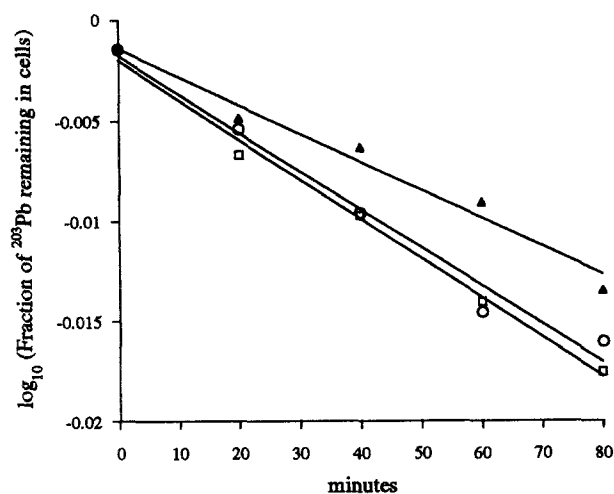
### Results of the two procedures

Figure 5 gives the results of studies of  $^{203}\text{Pb}$  equilibration, using both methods. The data are compared with observations made with fresh erythrocytes in autologous serum (Fig. 2), replotted against extracellular  $\text{Pb}^{2+}$  concentration, calculated as 1/5200 of the total  $\text{Pb}^{2+}$  concentration [1]. When the extracellular  $\text{Pb}^{2+}$  concentration is above 5 pM, erythrocyte  $^{203}\text{Pb}$  levels in the presence of ethylmaltol are very similar to those seen for fresh cells in serum, but about 2  $\mu\text{mol}/10^{13}$  cells higher than those seen in bicarbonate media. At  $\text{Pb}^{2+}$  concentrations below 5 pM significantly more  $^{203}\text{Pb}$  is found in erythrocytes suspended in serum than in medium under any conditions (Fig. 5B). Figure 5 also shows the effect of vanadate on  $^{203}\text{Pb}$  equilibration in a bicarbonate medium. Up to 20 pM  $\text{Pb}^{2+}$ , the cell  $^{203}\text{Pb}$  levels with vanadate closely parallel those seen with ethylmaltol, but at higher  $\text{Pb}^{2+}$  concentrations there is a precipitous rise in the amount of  $^{203}\text{Pb}$  associated with the cells. The reason for this was not investigated. It was not possible to use vanadate and ethylmaltol together, because they react chemically, and vanadate had no effect in serum, probably for similar reasons.

It is possible to estimate intracellular free  $\text{Pb}^{2+}$  concentrations from some of this data. The combined results for blood-bank cells equilibrated with ethylmaltol and fresh cells suspended in serum can be fitted either by a straight line through the origin, of slope 67.5  $\text{nmol} (10^{13} \text{ cells})^{-1} (\text{pM} \text{Pb}^{2+})^{-1}$  (not shown) or by a combination of a straight line and a saturation function, drawn on Fig. 5. If one assumes (a) that this curve represents the

equilibrium of  $\text{Pb}^{2+}$  across the plasmalemma according to the Nernst equation and (b) that membrane binding of  $^{203}\text{Pb}$  can be neglected (see below), one can obtain intracellular  $\text{Pb}^{2+}$  concentrations by multiplying the  $x$ -axis by 1.49, the approximate factor needed to correct for the negative intracellular membrane potential [16]. The relationship between cell  $^{203}\text{Pb}$  content and intracellular  $\text{Pb}^{2+}$  concentrations can be described as a combination of a linear component of slope 31  $\text{nmol} (10^{13} \text{ cells})^{-1} (\text{pM} \text{Pb}^{2+})^{-1}$  together with a high-affinity saturable component of  $4.5 \pm 2.5 \mu\text{mol} \text{Pb}/10^{13} \text{ cells}$  with a  $K_d$  of  $30 \pm 3 \text{ pM}$ . This model implies that a  $\text{Pb}^{2+}$  content of 1  $\mu\text{mol}/10^{13}$  cells corresponds to an intracellular free  $\text{Pb}^{2+}$  concentration of 6.5 pM, and 2  $\mu\text{mol}/10^{13}$  cells to 15.4 pM.

Figure 5 also includes data from experiments with ATP-depleted cells that were preincubated with inosine and iodoacetamide. The results by the two methods (bicarbonate and ethylmaltol equilibration) were indistinguishable and have been combined for clarity. Surprisingly,  $^{203}\text{Pb}$  uptake at steady state was very much less in these cells than in ATP-fed erythrocytes. Subsidiary experiments (not shown) showed this was not due to a reduced initial  $^{203}\text{Pb}$  uptake rate. The relationship between cellular  $^{203}\text{Pb}$  and extracellular  $\text{Pb}^{2+}$  concentration is linear, with a slope of 14.8  $\text{nmol} (10^{13} \text{ cells})^{-1} (\text{pM} \text{ extracellular} \text{Pb}^{2+})^{-1}$  (Fig. 5 B), equivalent to 9.9  $\text{nmol} (10^{13} \text{ cells})^{-1} (\text{pM} \text{ intracellular} \text{Pb}^{2+})^{-1}$ . A Pb content of 1  $\mu\text{mol}/10^{13}$  cells would correspond to an estimated intracellular free  $\text{Pb}^{2+}$  concentration of 101 pM, in ATP-depleted cells.



**Fig. 6.**  $^{203}\text{Pb}$  efflux from human erythrocytes. Cells were pre-incubated with  $^{203}\text{Pb}$  (standard medium with  $20\ \mu\text{M Pb}(\text{NO}_3)_2 + 1\ \text{mM NTA}$ ,  $25\ \text{mM HCO}_3^-$ ,  $5\ \text{mM glucose}$  and  $5\ \text{mM inosine}$ ,  $2\ \text{h}$  at  $37^\circ\text{C}$ ) to a level of  $1.5\ \mu\text{mol}/10^{13}$  cells, then washed and resuspended in standard medium at  $5\%$  haematocrit at  $37^\circ\text{C}$ . Duplicate samples were taken at each time:  $\circ$ , control conditions;  $\blacktriangle$ , efflux in the presence of  $2\ \text{mM vanadate}$ ;  $\square$ , efflux in the presence of  $10\ \mu\text{M DIDS}$ . Linear regression lines have slopes corresponding to efflux rate constants ( $\text{h}^{-1}$ ,  $\pm\ \text{SD}$ ) of  $0.027 \pm 0.002$  (control,  $\circ$ ),  $0.020 \pm 0.002$  (vanadate,  $\blacktriangle$ ),  $0.027 \pm 0.003$  (DIDS,  $\square$ )

#### Binding of $\text{Pb}^{2+}$ to ethylmaltol

Some of the  $^{203}\text{Pb}$  bound to erythrocytes might be present as a  $\text{Pb}$ -ethylmaltol complex. In order to assess this, the binding of  $\text{Pb}^{2+}$  by ethylmaltol dissolved in  $80\ \text{mM NaClO}_4$  and  $20\ \text{mM HEPES/KOH}$  ( $\text{pH } 7.4$ ) was studied by titration with a  $\text{Pb}(\text{NO}_3)_2$  solution, measuring the  $\text{Pb}^{2+}$  concentration with a  $\text{Pb}^{2+}$  electrode, as described previously [1].  $1\ \text{mM ethylmaltol}$  solution bound  $500\ \mu\text{M Pb}^{2+}$ , following a simple Langmuir isotherm with  $K_d = 260\ \text{nM}$  (not shown). This suggests the predominant formation of  $\text{Pb}(\text{ethylmaltol})_2$ . Its concentration is calculated to be  $19\ \text{nM}$  at  $10\ \text{pM Pb}^{2+}$  and  $0.5\ \mu\text{M}$  at  $250\ \text{pM Pb}^{2+}$ , in  $1\ \text{mM ethylmaltol}$  solutions.

#### $^{203}\text{Pb}$ efflux from erythrocytes

When erythrocytes are loaded with small amounts of  $^{203}\text{Pb}$ , washed, and resuspended in  $^{203}\text{Pb}$ -free medium at  $37^\circ\text{C}$ , the rate of loss of  $^{203}\text{Pb}$  is partly inhibited by  $4\ \text{mM vanadate}$ , but not affected by  $10\ \mu\text{M DIDS}$  (Fig. 6).

$^{203}\text{Pb}$  efflux rate constants can be calculated from the slopes of the lines drawn in Fig. 6. These were quite variable, but a good correlation was obtained between the vanadate-sensitive  $^{203}\text{Pb}$  efflux and cellular  $^{203}\text{Pb}$  content (Fig. 7). If this represents  $\text{Ca}^{2+}$  pump activity, one would expect it to be zero in ATP-depleted cells. However, vanadate appeared to stimulate  $^{203}\text{Pb}$  efflux in ATP-depleted cells, i. e. the vanadate-sensitive flux was negative (Fig. 7). The intracellular binding of  $\text{Pb}^{2+}$  is much smaller in ATP-depleted cells (Fig. 5), so these

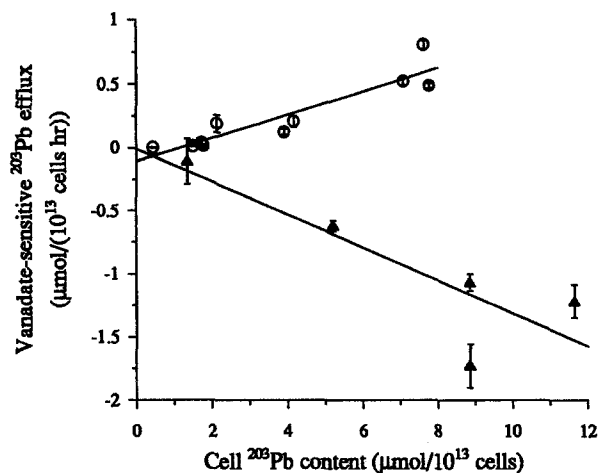


**Fig. 7.** Vanadate-sensitive  $^{203}\text{Pb}$  efflux and cellular  $^{203}\text{Pb}$  content. The reduction in  $^{203}\text{Pb}$  efflux caused by  $2\ \text{mM vanadate}$  is plotted against the cell  $^{203}\text{Pb}$  content at the start of the efflux incubation, for ATP-fed ( $\circ$ ) and ATP-depleted cells ( $\blacktriangle$ ) ( $\pm\ \text{SD}$ ). Cells were depleted of ATP by the inclusion of  $5\ \text{mM inosine}$  and  $5\ \text{mM iodoacetamide}$  in the  $^{203}\text{Pb}$  loading preincubation. Linear regression lines have been drawn. For an analysis in terms of estimated intracellular  $\text{Pb}^{2+}$  concentration, please see the text

cells actually have larger intracellular  $\text{Pb}^{2+}$  concentrations than the ATP-fed cells.

Figure 7 could also be presented as a graph of vanadate-sensitive  $^{203}\text{Pb}$  efflux against estimated intracellular free  $\text{Pb}^{2+}$  concentration, using the calibration derived in Fig. 5. If this is done, the graphs are linear through the origin (not shown), with slopes  $+4.8 \pm 0.6\ \text{nmol } (10^{13}\ \text{cells})^{-1}\ \text{h}^{-1} (\text{pM Pb}^{2+})^{-1}$ , for ATP-fed cells, and  $-1.3 \pm 0.5\ \text{nmol } (10^{13}\ \text{cells})^{-1}\ \text{h}^{-1} (\text{pM Pb}^{2+})^{-1}$ , for ATP-depleted cells (both  $\pm\ \text{SD}$ ).

#### Membrane binding of $^{203}\text{Pb}$

Erythrocyte membranes (“white ghosts”) were prepared as described previously [4], but two attempts to study the binding of  $^{203}\text{Pb}$  with  $\text{Pb/NTA}$  buffers (free  $\text{Pb}^{2+}$  in the range  $2\text{--}100\ \text{pM}$ ) were unsuccessful, in the sense that  $^{203}\text{Pb}$  was excluded by the membranes so that its concentration in the membrane fraction was lower than in the supernatant fraction.

#### Discussion

When human erythrocytes are suspended in serum or in  $\text{Pb}^{2+}$  buffers, and allowed to take up  $1\text{--}5\ \mu\text{mol } ^{203}\text{Pb}/10^{13}\ \text{cells}$ , this uptake appears to represent transport across the cell membrane and into a cytoplasmic pool, and not binding to the membrane.  $^{203}\text{Pb}$  uptake is sensitive to DIDS when erythrocytes are suspended in serum or in standard medium. In medium, it is bicarbonate-dependent, indicating that it occurs via the anion exchanger [14]. The initial rate of  $^{203}\text{Pb}$  uptake at  $20\ \text{pM Pb}^{2+}$  is about  $1\ \mu\text{mol } (10^{13}\ \text{cells})^{-1}\ \text{h}^{-1}$  (Fig. 3), which is quantitatively comparable to rates measured previously

at 1000-fold higher concentrations [13]. DIDS does not completely block  $^{203}\text{Pb}$  uptake for fresh erythrocytes in serum (Fig. 1), suggesting that there may also be another  $\text{Pb}^{2+}$  influx pathway. Small  $\text{Pb}^{2+}$  influxes and effluxes were seen in earlier work in the presence of DIDS [14]. Their nature remains unknown. Vanadate stimulates  $^{203}\text{Pb}$  uptake in medium (Fig. 3), enhances the steady-state level of  $^{203}\text{Pb}$  in the cells (Fig. 5) and inhibits  $^{203}\text{Pb}$  efflux (Fig. 6), all of which suggest that the  $\text{Ca}^{2+}$  pump contributes to  $\text{Pb}^{2+}$  efflux. However, this route accounts for less than 50% of the efflux (Fig. 6) and is quantitatively much smaller than seen in resealed erythrocyte ghosts [15]. The extrapolated rate in ghosts as  $[\text{Pb}^{2+}]$  approaches zero is  $13.8 \text{ mmol (l cells)}\text{h}^{-1}$  divided by  $47 \text{ nM}$  [15], equivalent to  $235 \text{ nmol (}10^{13} \text{ cells)}^{-1} \text{ h}^{-1}$  ( $\text{pM Pb}^{2+}$ ) $^{-1}$ , assuming a mean cell volume of 80 fl. This compares with an estimated rate of  $5 \text{ nmol (}10^{13} \text{ cells)}^{-1} \text{ h}^{-1}$  ( $\text{pM Pb}^{2+}$ ) $^{-1}$  in the present experiments (Fig. 7). The reason for this discrepancy is not clear; it may relate to differences in calmodulin content between erythrocytes and ghosts.

No membrane binding of  $^{203}\text{Pb}$  could be detected at  $\text{Pb}^{2+}$  concentrations up to 100 pM. Earlier observations with a  $\text{Pb}^{2+}$  electrode found 100–200  $\mu\text{mol}/10^{13}$  cells for  $\text{Pb}^{2+}$  binding at 1  $\mu\text{M Pb}^{2+}$  [14], equivalent to  $0.1\text{--}0.2 \text{ nmol(}10^{13} \text{ cells)}^{-1}$  ( $\text{pM Pb}^{2+}$ ) $^{-1}$ , assuming there is no additional high-affinity component of  $\text{Pb}^{2+}$  binding to membranes. This is smaller than the steady-state  $^{203}\text{Pb}$  content of ATP-depleted cells:  $1.5 \text{ nmol(}10^{13} \text{ cells)}^{-1}$  ( $\text{pM Pb}^{2+}$ ) $^{-1}$  (Fig. 5), suggesting that most of the cellular  $^{203}\text{Pb}$  is cytoplasmic. The linearity of the relationship between cell  $^{203}\text{Pb}$  content and  $\text{Pb}^{2+}$  concentration in ATP-depleted cells makes a high-affinity pool of membrane-bound  $\text{Pb}^{2+}$  unlikely.

The steady-state measurements of the relationship between cellular  $^{203}\text{Pb}$  content and extracellular  $\text{Pb}^{2+}$  concentration (Figs. 2 and 5) are subject to a number of reservations. Insufficient time may have been allowed for equilibration at the lowest  $\text{Pb}^{2+}$  concentrations. This may account for the sigmoid relationship between cell  $^{203}\text{Pb}$  content and extracellular  $\text{Pb}^{2+}$  concentration seen in some of the conditions in Fig. 5B. No allowance was made for pre-existing cell  $\text{Pb}^{2+}$ , although isolated observations (reported above) suggest this was negligible. Different methods were used to study the relationship between cell  $^{203}\text{Pb}$  content and extracellular  $\text{Pb}^{2+}$  concentration, because of the possibility that the steady-state might reflect the balance between influx and an outwardly directed pump. The working hypothesis was that the pump could be overcome either by the use of vanadate, to inhibit it, or by ethylmaltol, which acts as a  $\text{Pb}^{2+}$  ionophore. The results at  $\text{Pb}^{2+}$  concentrations up to 20 pM (Fig. 5B) seem to support this, with coincident results for vanadate and ethylmaltol, considerably greater than the  $^{203}\text{Pb}$  levels seen with bicarbonate. However, at higher  $\text{Pb}^{2+}$  concentrations, vanadate gives exponentially rising cell  $^{203}\text{Pb}$  levels. This might be related to the formation of an insoluble Pb-vanadate complex. The difference between the cell  $^{203}\text{Pb}$  level with ethylmaltol and bicarbonate is quite marked at low  $\text{Pb}^{2+}$  concentrations, but not at high. At 240 pM  $\text{Pb}^{2+}$  the differ-

ence is  $3.7 \pm 2.6 \mu\text{mol}/10^{13}$  cells (Fig. 5A). This might be accounted for by the binding of  $\text{Pb(ethylmaltol)}_2$ , which is calculated to have a concentration of 0.5  $\mu\text{M}$  at this  $\text{Pb}^{2+}$  concentration. Furthermore, the results with erythrocytes suspended in serum agree well with those with ethylmaltol (Fig. 5), yet if there were significant pumping activity, one would expect there to be more  $^{203}\text{Pb}$  in the cells with ethylmaltol. Taken together with the relatively small vanadate-sensitive  $^{203}\text{Pb}$  efflux, these observations suggest that the pump component is small, and the  $\text{Pb}^{2+}$  distribution is close to equilibrium for human erythrocytes in blood under physiological and pathological circumstances.

The most striking feature of the steady-state data (Fig. 5) is the large component of cytoplasmic  $\text{Pb}^{2+}$  binding that disappears when the cells are depleted of ATP by preincubation with inosine and iodoacetamide. This labile component amounts to over 90% of the total binding for cell  $\text{Pb}^{2+}$  contents up to 2  $\mu\text{mol}/10^{13}$  cells (Fig. 5B). It appears to be largely responsible for the high proportion of blood  $\text{Pb}^{2+}$  found in the erythrocytes [4, 9]. The labile  $\text{Pb}^{2+}$  binding may include a small high-affinity component, fitted by a curve on Fig. 5. It is unlikely to be due to Haemoglobin [2] because a linear fit to the data has a slope of  $45 \text{ nmol (}10^{13} \text{ cells)}^{-1}$  ( $\text{pM intracellular Pb}^{2+}$ ) $^{-1}$  in ATP-fed cells, while earlier measurements of  $\text{Pb}^{2+}$  binding to haemoglobin in dialysed erythrocyte lysates with a  $\text{Pb}^{2+}$  electrode found 20  $\mu\text{mol bound Pb (g protein)}^{-1}$  ( $\mu\text{M Pb}^{2+}$ ) $^{-1}$  [14], equivalent to  $5 \text{ nmol (}10^{13} \text{ cells)}^{-1}$  ( $\text{pM Pb}^{2+}$ ) $^{-1}$ , assuming 250 g haemoglobin/ $10^{13}$  cells. It is also unlikely to be due to ATP. The  $K_d$  for Pb-ATP has been reported to be 22  $\mu\text{M}$  [18], but a value of 0.2  $\mu\text{M}$  has been measured with the  $\text{Pb}^{2+}$  electrode at pH 7.3 (Simons, unpublished). A 1 mM solution of ATP (approximate intracellular concentration) would bind 5 nmol Pb ( $10^{13} \text{ cells)}^{-1}$  ( $\text{pM intracellular Pb}^{2+}$ ) $^{-1}$ , taking the 0.2  $\mu\text{M}$  value for the  $K_d$ , or 1/100 of that, taking the 22  $\mu\text{M}$  value. The nature of the labile  $\text{Pb}^{2+}$ -binding has yet to be determined – it may be a specific  $\text{Pb}^{2+}$ -binding protein [11], and it could also relate to the observation that the majority of  $^{210}\text{Pb}$  in  $^{210}\text{Pb}$ -loaded erythrocytes is bound to components of lower molecular mass than haemoglobin [3].

A quantitative comparison can also be made with earlier observations that the ratio of plasma  $\text{Pb}^{2+}$  to erythrocyte  $\text{Pb}^{2+}$  is 0.74% in  $\text{Pb}^{2+}$ -exposed humans [9] and the ratio of serum  $\text{Pb}^{2+}$  to blood  $\text{Pb}^{2+}$  is 0.83% in control humans [4]. An extracellular  $\text{Pb}^{2+}$  concentration of 2 pM would correspond to a serum  $\text{Pb}^{2+}$  concentration of 10.5 nM (using a bound/free ratio of 5200 [8]), and to a cellular  $\text{Pb}^{2+}$  content of 0.5  $\mu\text{mol}/10^{13}$  cells (fitted curve on Fig. 5B), equivalent to 0.625  $\mu\text{mol/l}$  cells, assuming a mean cell volume of 80 fl. The predicted ratio of serum  $\text{Pb}^{2+}$  to erythrocyte  $\text{Pb}^{2+}$  would thus be 1.7%, about twice the value seen in vivo. There is no obvious explanation for this discrepancy: one possibility may be that the bound/free  $\text{Pb}^{2+}$  ratio in serum was measured at 25°C [1], rather than at 37°C.

Another comparison with earlier work can be made.  $\text{Pb}^{2+}$  stimulates  $\text{K}^+$  efflux from human erythrocytes [6].

This effect has a threshold, which has been reported to be about 36 nmol Pb/g cells [6]. This is equivalent roughly to 40  $\mu\text{mol/l}$  cells or 32  $\mu\text{mol}/10^{13}$  cells. This is beyond the range of observations reported in the current paper, but if the curve fitted in Fig. 5 is valid at higher  $\text{Pb}^{2+}$  concentrations, calculations show that 32  $\mu\text{mol}/10^{13}$  cells is equivalent to an estimated intracellular free  $\text{Pb}^{2+}$  concentration of 0.9 nM. This is exactly the same as the threshold for the stimulation of  $^{86}\text{Rb}$  efflux from human erythrocyte ghosts by intracellular  $\text{Pb}^{2+}$  buffers [13].

*Acknowledgement.* This work was supported by the Wellcome Trust (UK).

## References

1. Al-Modhefer AJA, Bradbury MWB, Simmons TJB (1991) Observations on the chemical nature of lead in human blood serum. *Clin Sci* 81:823–829
2. Barltrop D, Smith A (1971) Interaction of lead with erythrocytes. *Experientia* 27:92–93
3. Barton JC (1989) Retention of radiolabel by human erythrocytes in vitro. *Toxicol Appl Pharmacol* 99:314–322
4. DeSilva PE (1981) Determination of lead in plasma and studies on its relationship to lead in erythrocytes. *Br J Ind Med* 38:209–217
5. Glynn IM, Lew VL, Lüthi U (1971) Reversal of the potassium entry mechanism in red cells, with and without reversal of the active pump cycle. *J Physiol (Lond)* 207:371–391
6. Grigarzik H, Passow H (1958) Versuche zum Mechanismus der Bleiwirkung auf die Kaliumpermeabilität roter Blutkörperchen. *Pflügers Arch* 267:73–92
7. Hider RC, Ejim L, Taylor PD, Gale R, Huehms E, Porter J (1990) Facilitated uptake of zinc into human erythrocytes. Relevance to the treatment of sickle-cell anaemia. *Biochem Pharmacol* 39:1005–1012
8. Mahaffey KR (1990) Environmental lead toxicity: nutrition as a component of intervention. *Environ Health Perspect* 89:75–78
9. Manton WI, Cook JD (1984) High accuracy (stable isotope dilution) measurements of lead in serum and cerebrospinal fluid. *Br J Ind Med* 41:313–319
10. Martell AE, Smith RM (1974) Critical stability constants. Plenum Press, New York
11. Raghavan SRV, Culver BD, Gonick HC (1980) Erythrocyte lead-binding protein after occupational exposure: I. Relationship to lead toxicity. *Environ Res* 22:264–270
12. Simons TJB (1984) Active transport of lead by human red blood cells. *FEBS Lett* 172:250–254
13. Simons TJB (1985) Influence of lead ions on cation permeability in human red cell ghosts. *J Membr Biol* 84:61–71
14. Simons TJB (1986) Passive transport and binding of lead by human red blood cells. *J Physiol (Lond)* 378:267–286
15. Simons TJB (1988) Active transport of lead by the calcium pump in human red cells ghosts. *J Physiol (Lond)* 405:105–113
16. Simons TJB (1991) Intracellular free zinc and zinc buffering in human red blood cells. *J Membr Biol* 123:63–71
17. Simons TJB (1992) Lead transport and binding by human red blood cells at “physiological” lead levels (abstract). *J Physiol (Lond)* 446:175P
18. Tice LW (1969) Lead-adenosine triphosphate complexes in adenosine triphosphatase histochemistry. *J Histochem Cytochem* 17:85–94